Journal of Advanced Research 24 (2020) 379–389

Contents lists available at ScienceDirect

Journal of Advanced Research

journal homepage: www.elsevier.com/locate/jare

Exciplex energy transfer through spacer: White electroluminescence with enhanced stability based on cyan intermolecular and orange intramolecular thermally activated delayed fluorescence

Galyna Sych [a], Matas Guzauskas [a], Dmytro Volyniuk [a], Jurate Simokaitiene [a], Hryhorii Starykov [b], Juozas V. Grazulevicius [a,*]

[a] Department of Polymer Chemistry and Technology, Kaunas University of Technology, Barsausko 39, LT- 51423 Kaunas, Lithuania
[b] Ivan Franko National University of Lviv, Kyryla I Mefodiya, 6, Lviv 79005, Ukraine

GRAPHICAL ABSTRACT

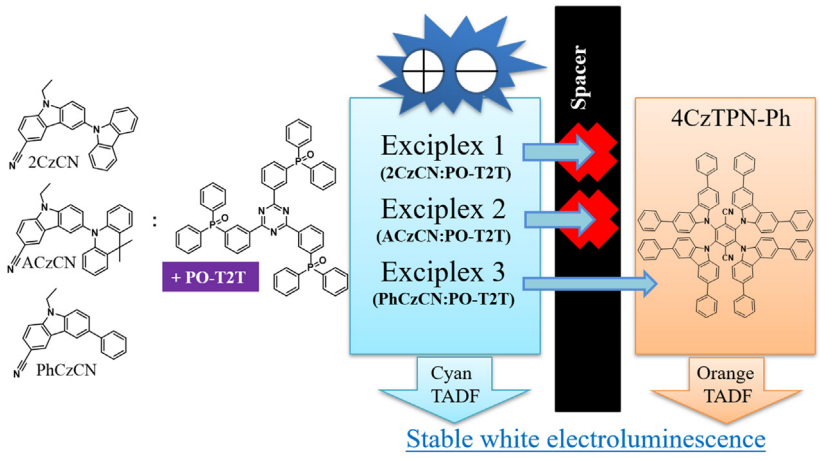

ARTICLE INFO

Article history:
Received 10 February 2020
Revised 9 April 2020
Accepted 26 April 2020
Available online 16 May 2020

Keywords:
Thermally activated delayed fluorescence
Exciton energy transfer
Exciplex
White OLED

ABSTRACT

Capability of exciplex energy transfer through a spacer was investigated using three exciplex-forming solid mixtures which contained the well-known electron accepting 2,4,6-tris[3-(diphenylphosphinyl)phenyl]-1,3,5-triazine and appropriately designed bipolar cyanocarbazolyl-based derivatives functionalized by attachment of carbazolyl, acridanyl or phenyl units. These novel cyanocarbazolyl-based derivatives were used as both the spacer and exciplex-forming donor. Efficient organic light-emitting diodes with electroluminescence in cyan-yellow region and maximum external quantum efficiency of up to 7.7% were fabricated owing to efficient thermally activated fluorescence (TADF) of the newly discovered exciplexes. An approach of exciton separation by the spacer between the studied exciplexes and selected orange TADF emitter was proposed for the fabrication of white electroluminescent devices with prolonged lifetime comparing to that of single-color exciplex-based devices. Exciplex-forming systems were tested for exciton separation between inter- and intramolecular TADF. Exciplex energy transfer through a spacer was observed on relatively long distance for one system due to the energy resonance between triplet

Peer review under responsibility of Cairo University.
* Corresponding author.
E-mail address: juozas.grazulevicius@ktu.lt (J.V. Grazulevicius).

https://doi.org/10.1016/j.jare.2020.04.018
2090-1232/© 2020 THE AUTHORS. Published by Elsevier BV on behalf of Cairo University.
This is an open access article under the CC BY-NC-ND license (http://creativecommons.org/licenses/by-nc-nd/4.0/).

levels of the exciplex and spacer. First time observed here exciplex energy transfer through a spacer can be useful for both improvement of device stability and obtaining of white electroluminescence.
© 2020 THE AUTHORS. Published by Elsevier BV on behalf of Cairo University. This is an open access article under the CC BY-NC-ND license (http://creativecommons.org/licenses/by-nc-nd/4.0/).

Introduction

Exciplex formation is useful approach to obtain thermally activated delayed fluorescence (TADF) by simple mixing of organic electron-donating and electron-accepting molecules [1,2]. Organic semiconductors with TADF properties are vitally required by organic electronics industry since they allow to harvest usually non-emissive triplet states through reverse intersystem crossing (RISC) [3]. Usage of TADF materials as emitters and/or hosts allows to increase the internal quantum efficiencies (IQEs) up to 100% of organic light-emitting diodes (OLEDs) and light-emitting electrochemical cells and to avoid utilization of materials based on rare earth elements [4,5]. One more advantage of TADF emitters versus phosphorescent emitters is a possibility to fabricate highly efficient non-doped OLEDs, while emission of non-doped films of phosphorescent emitters is always quenched [6]. Single-color OLEDs with EQE values slightly higher than 20% were recently obtained using green-yellow exciplex-forming systems [7,8] as well as new OLED fabrication approaches (utilizing of a tricomponent exciplex emitter, for example) [9,10]. The highest EQE of 24% was obtained for green ternary exciplex emission-based devices fabricated by solution processing which was not much lower than EQEs of the best green OLEDs based on intramolecular TADF or phosphorescent emitters [11]. However, maximum EQE values of sky-blue/deep-blue exciplex based devices are significantly lower than above mentioned state-of-art green OLEDs [12,13]. Cyan exciplex emission-based OLEDs with maximum EQE of 16% was obtained using a cyanocarbazolyl-based derivative as donor which formed exciplex with 2,4,6-tris[3-(diphenylphosphinyl)phenyl]-1,3,5-triazine (PO-T2T) [14]. Exciplex-based emitters were also used for the fabrication of white electroluminescent (EL) devices since they are characterized by broad emission spectra with full width at half maxima (FWHM) exceeding of 100 nm [15,16]. All-exciplex based devices were developed by mixing of blue and orange TADF exciplex emissions under electrical excitation in well-designed device structures [13]. Efficient "warm-white" OLEDs were fabricated using bicarbazole-based blue TADF emitter 4,4′-(9*H*,9′*H*-[3,3′-bicarbazole]-9,9′-diyl)bis(3-(trifluoromethyl)benzonitrile) which additionally formed orange emitting exciplex with a selected donor [17]. White electroluminescence was also observed be employing volume and interface exciplexes as host and emitter together with the fluorescent dye [18]. In above mentioned exciplex emission-based approaches for white OLEDs, charge recombination and exciton recombination zones were distributed between different emitters of the devices with one or two light-emitting layers. For the reduction of energy losses due to energy transfer and triplet–triplet annihilation, separation of charge recombination and exciton recombination zones between blue fluorescence and yellow phosphorescent emitters were proposed earlier for high-efficiency fluorescent/phosphorescent hybrid OLEDs [19]. In such white OLEDs, singlet excitons were harvested in the layer of blue fluorescent emitter while triplet excitons with the higher diffusion length than that of singlets where transferred to orange phosphorescent emitter. Since direct harvesting of triplet excitons through the RISC takes place in TADF emitters [3], long-distance (longer distance than that required for the long-range Förster energy transfer (FRET)) energy transfer from one TADF emitter to another one is not expected. In contrast to this expectation, we observed separation of charge recombination and exciton recombination zones between two TADF emitters (intermolecular and intramolecular ones) detecting exciplex energy transfer through spacer (Fig. 1).

When exciplex-forming donor and exciplex-forming acceptor are separated by inert spacer, long-distance exciplex or even ultra-long-distance exciplex can be formed [20,21]. It is not case of the studied TADF-based systems since volume exciplex were formed in one layer then its energy was transferred through the spacer to another TADF-based layer. Exciplex-forming donor and exciplex-forming acceptor were not separated by the spacer in the studied TADF-based systems (Fig. 1). The differences between conventional TADF-based systems and the studied TADF/spacer/exciplex systems are briefly described below. When the distance between sensitizing TADF host and (TADF) emitter is small enough for the long-range Förster energy transfer as well as when triplet energy differences between conventional host and sensitizing TADF host is high enough for preventing triplet energy transfer, it is the case of conventional TADF-based systems. Such conventional TADF-based systems including exciplex-based ones are usually based on the doped host:sensitizer:guest systems [22,23], bilayer systems [12,24], and rare examples of multilayered spacer-based conventional TADF-based systems [25] were also published. When the distance between sensitizing TADF emitter and TADF emitter is too high for FRET and when triplet energy differences between sensitizing TADF emitter and spacer is low enough for allowing triplet energy transfer, it is the case of the studied TADF-based systems.

In this work, we propose an approach to appropriately distribute excitons between exciplex-based cyan and orange emitters both exhibiting efficient thermally activated delayed fluorescence to obtain "stable" white electroluminescence. Excitons are generated in an exciplex-based light-emitting layer under electrical excitation and are transferred to 2,3,5,6-tetrakis (3,6-diphenyl-9*H*-carbazol-9-yl)-1,4- benzenedicarbonitrile (4CzTPN-Ph) [26] as it is schematically shown in Fig. 1. For this purpose, new series of cyanocarbazolyl derivatives 2CzCN, ACzCN, and PhCzCN were synthesized and characterized as exciplex-forming materials. The synthesized compounds were found to be capable to form efficient exciplexes with commercially available electron-withdrawing compound PO-T2T (Fig. 1). Exciplex energy transfer through a spacer was detected only for one studied exciplex-forming solid mixture. It was caused by energy resonance between triplet levels of the exciplex PhCzCN:PO-T2T and spacer PhCzCN (Fig. 1).

Experimental section

Materials

Commercially available hexaazatriphenylenehexacabonitrile (HAT-CN), tris(4-carbazoyl-9-ylphenyl)amine (TCTA), 2,3,5,6-*tetrakis*(3,6-diphenyl-9*H*-carbazol-9-yl)-1,4- benzenedicarbonitrile (4CzTPN-Ph), bis(1-phenyl-isoquinoline-C2,N)(acetylacetonato)iridium(III) (Ir(piq)$_2$ (acac)), 2,4,6-tris[3-(diphenylphosphinyl)phenyl]-1,3,5-triazine (PO-T2T), 2,2′,2′′-(1,3,5-benzinetriyl)-tris(1-phenyl-1-H-benzimidazole) (TPBi), fluorolithium (LiF) were purchased from Sigma-Aldrich and used as received.

The starting materials i.e. 9*H*-carbazole, sodium *tert*-butoxide, *tetrakis*-triphenylphosphine palladium (Pd(PPh$_3$)$_4$), ethyl bromide, glacial acetic and sulfuric acids, copper (Cu), potassium iodide (KI), potassium iodate (KIO_3), sodium hydroxide (NaOH),

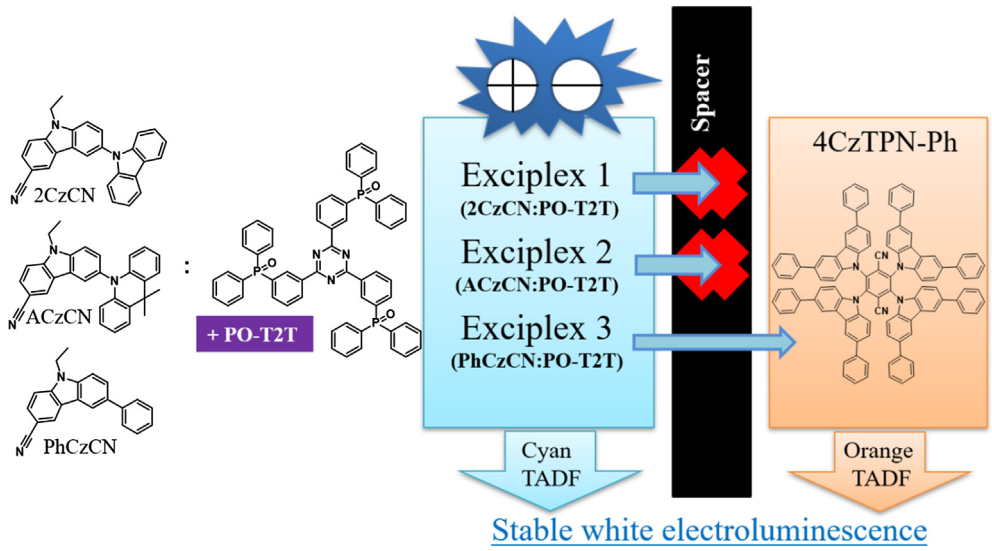

Fig. 1. Chemical structures of exciplex-forming materials (2CzCN, ACzCN, PhCzCN, and PO-T2T used respectively as donors and acceptor) and visualization of the exciplex energy transfer through a spacer which occurred for exciplex PhCzCN:PO-T2T (exciplex 3).

potassium carbonate (K_2CO_3), anhydrous sodium sulfate (Na_2SO_4), potassium hydroxide (KOH), copper cyanide (CuCN), 18-crown-6, and 1,2-dichlorobenzene were purchased from Sigma-Aldrich and used as received. 9-Ethyl-9*H*-carbazole was synthesized according to the previously reported procedure [27]. 9-Ethyl-3,6-diiodo-9*H*-carbazole was obtained similarly to the known procedure [28]. Synthetic procedures and the structural characterization of the cyanocarbazolyl derivatives are described in Supporting Information.

In addition, procedures of the provided experiments are presented in Supporting Information (see section Instrumentation).

Results and discussions

Synthetic procedure

Compounds 2CzCN, ACzCN and PhCzCN were obtained by the synthetic routes shown in Scheme 1. In the first step alkylation of 9-*H* carbazole afforded 9-ethyl-carbazole. Iodinated at C-3 and C-6 position carbazole derivative was obtained by the action of KI and KIO_3 in glacial acetic acid solution on the alkylated carbazole according to the Tucker iodination reaction [22]. The next step copper-catalyzed Ullmann coupling reaction of carbazole or acridane and 3,6-di-iodocarbazole afforded monosubstituted intermediate compounds 2CzI and ACzI. Palladium-catalyzed Suzuki cross-coupling reaction of phenyl boronic acid and the corresponding halides was used to obtain monosubstituted intermediate compound PhCzI. In the final step, Rosenmund-von Braun reaction of intermediate halides with an excess of copper (I) cyanide in a polar boiling DMF solvent afforded target compounds in moderate yields (Scheme 1).

Common characterization

Thermal Properties. The thermal properties of the compounds were evaluated by differential scanning calorimetry (DSC) and thermogravimetric analysis (TGA). The highest temperature of 5% weight loss ($T_{d\text{-}5\%}$) was observed for bi-carbazolyl-based compound 2CzCN (Fig. 2a). Its $T_{d\text{-}5\%}$ was found to exceed 350 °C. Compounds 2CzCN, ACzCN and PhCzCN were obtained after the synthesis and purification as crystalline substances. All three target compounds exhibited endothermic melting signals during the first heating scans with melting temperatures ranging from 133 to 253 °C (Table 1). The melting temperatures values of compounds strongly depend on the size of the molecules. Thus, ACzCN with the highest molecular weight exhibited the highest T_m of 253 °C, meanwhile the smallest PhCzCN showed the lowest T_m of 133 °C (Fig. S1). During the second heating scan 2CzCN and PhCzCN form molecular glasses with glass-transition temperatures (T_g) of 101 °C and 42 °C, respectively (Fig. S1, Table 1). Higher T_g value for 2CzCN in respect to PhCzCN is conceivably due to the higher molecular weight of the 2CzCN and thus stronger intermolecular interactions [29]. During the first cooling scan of ACzCN sample, crystallization peak was recorded (Fig. S1). Hence, no glass transition temperature was recorded during the following heating scan.

Electrochemical and photoelectrical properties. Electrochemical properties of 2CzCN, ACzCN and PhCzCN was evaluated by cyclic voltammetry (CV). All three compounds along the series exhibited irreversible oxidation and reduction processes (Fig. 2b). The substituent at C-6 position of 3-cyanocarbazole fragment highly influenced the energy levels of compounds. ACzCN exhibited the lowest ionization potential IP_{CV} of 5.33 eV along the series due to the extended π-conjugation and stronger electron-donating ability of acridan moiety in comparison with carbazolyl and phenyl side-substituents (Table 1). PhCzCN with its reduced extent of conjugation displayed the highest IP_{CV} value of 5.70 eV. Due to the presence of identical electron-withdrawing cyano groups, all three compounds were characterized with similar electron affinity (EA_{CV}) values of 2.22 eV. The ionization potential of the solid samples IP_{PE} were estimated from photoelectron emission (PE) spectra of vacuum deposited layers of the compounds (Fig. 2c). IP_{PE} values were found to be in the range of 5.80–6.12 eV (Table 1). The discrepancy of ionization potential values obtained from CV and PE spectra was expected due to the different environmental conditions (dilute DMF solutions and solid samples) [30].

Charge-transporting properties. Hole- and electron-transporting properties of the layers of compounds 2CzCN and ACzCN were studied by time of flight (TOF) method. The TOF transients of holes and electrons of thin layers of 2CzCN and ACzCN are shown in Fig. S2. According to these transients, compounds 2CzCN and ACzCN showed transport of holes and electrons of moderate dispersity. Due to the low molecular weight of PhCzCN fast crystallization was observed in its thick films. Therefore TOF measurements were impossible. Compounds **2CzCN** and **ACzCN**

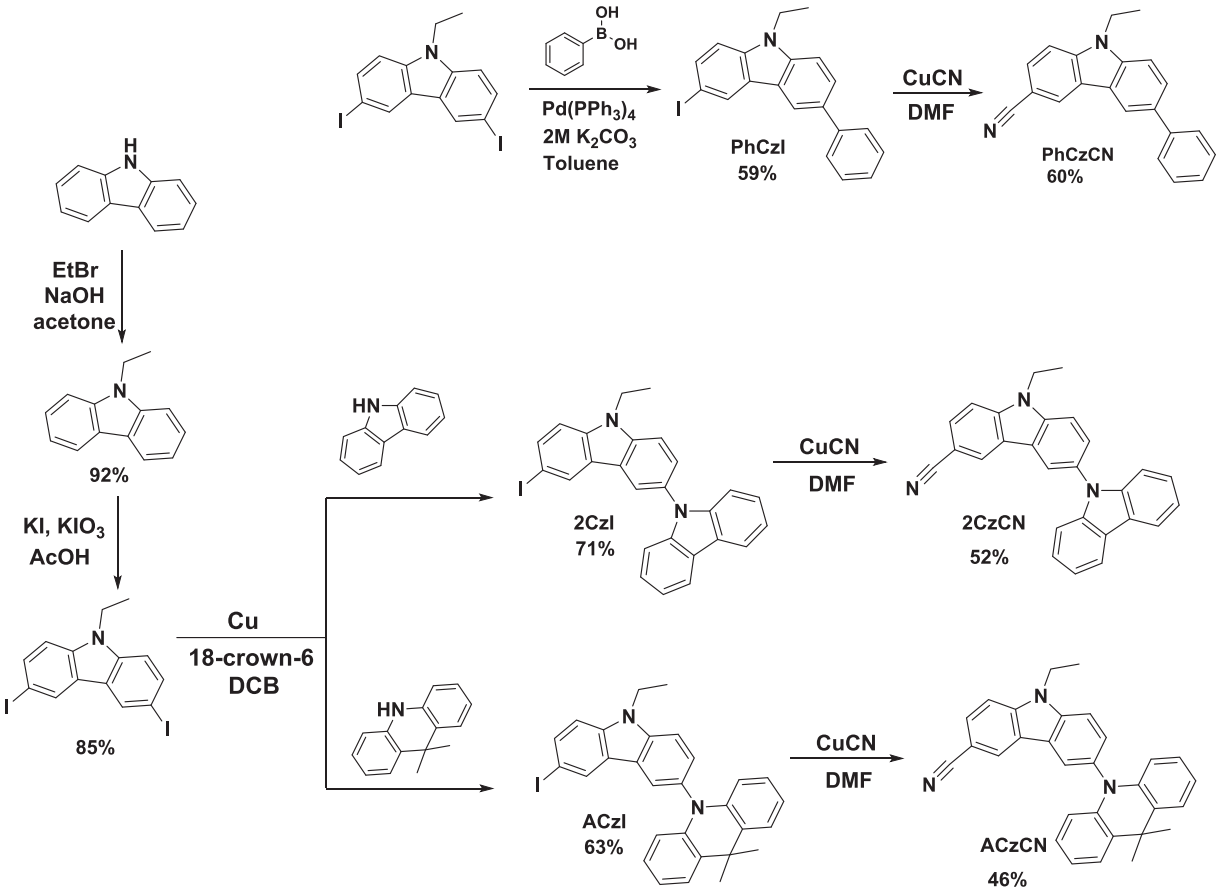

Scheme 1. Synthetic routes towards compounds 2CzCN, ACzCN, and PhCzCN.

exhibited relatively balanced transport of holes and electrons with slightly higher electron mobilities (Fig. 2d). Hole and electron mobilities for **2CzCN** were found to be of 4×10^{-5} $cm^2V^{-1}s^{-1}$ and 6.5×10^{-5} $cm^2V^{-1}s^{-1}$ at electric field of ca. 8.3×10^5 V cm^{-1}, respectively. The layer of **ACzCN** showed hole mobility of 4.9×10^{-5} $cm^2V^{-1}s^{-1}$ and electron mobility of 5.9×10^{-5} $cm^2V^{-1}s^{-1}$ at electric field of ca. 4.7×10^5 V cm^{-1}.

Photophysical properties. UV–vis spectra of the neat films of the studied compounds resembled those of their dilute toluene solutions (10^{-5} M) (Fig. 3a). The solid films of **2CzCN**, **PhCzCN** and **ACzCN** emitted light in the violet-deep blue region with the emission maxima peaks centered at 410 nm, 424 nm and 407 nm, respectively. Compound **PhCzCN** with the minor conjugation length of the phenyl substituted cyano carbazole moiety exhibited the most blue-shifted emission in both toluene solution and in solid state (Table 2). Toluene solutions of **2CzCN** and **PhCzCN** exhibited structured photoluminescence (PL) spectra with dual emission peaks. Such a resolved vibronic shapes of PL spectra are apparently due to the emission originating from recombination of locally excited carbazole moiety [31]. Toluene solutions and neat films of compound **ACzCN** displayed the most bathochromically shifted deep blue emission with maxima located at 422 and 424 nm, respectively. This emission behaviour of ACzCN in respect to 2CzCN and PhCzCN can be explained by the presence of strong electron-donating acridan unit linked to cyanocarbazolyl moiety. To evaluate the energies of excited states of compounds, phosphorescence and luminescence spectra were recorded at 77 K (Fig. 3b).

The values of the first excited singlet and triplet energy levels were determined from the onsets of luminescence and phosphorescence spectra respectively (Table 2). The studied cyano carbazolyl derivatives exhibited high first excited singlet state energies, explaining their violet-blue fluorescence (Table 2). All three compounds displayed intense broad well-resolved phosphorescence spectra, which, apparently is attributed to the local excitation of triplet state of carbazole fragment, similarly to previously reported other carbazole-based compounds [32,33]. Accordingly, the compounds were characterized with similar high energy of the first excited triplet states varying from 2.90 eV for **PhCzCN** to 3.03–3.04 eV for **2CzCN** and **ACzCN** (Table 3).

PL decay dynamics and photoluminescence quantum yields (PLQY) of all cyanocarbazolyl containing compounds were estimated at room temperature (Fig. S3, Table 2). PL decay curves of toluene solutions of the compounds were monoexponential, while their solid films exhibited biexponential character which may be related to the excitation migration towards the non-radiative decay sites [34] (Table 2). Fluorescence lifetimes of the solid samples of the compounds were found to be in nanoseconds range (4–10 ns). PLQY values estimated for neat films of the compounds ranged from 7% for acridan-containing **ACzCN** up to 15% for bi-carbazolyl based **2CzCN**. Compound **PhCzCN** with phenyl side substituent demonstrated PLQY of 11% (Table 2). The lowest PLQY value for acridan-based **ACzCN** can be assigned to the diminution of the conjugation between cyano carbazolyl and acridan moieties.

Exciplex-forming properties

The synthesized bipolar cyanocarbazolyl-containing compounds were tested as the electron-donating materials for the formation of excited complexes with electron-withdrawing commercially available PO-T2T. Electron-transporting PO-T2T was selected due to its excellent thermal stability, high triplet state energy and high LUMO energy favorable for exciplex formation

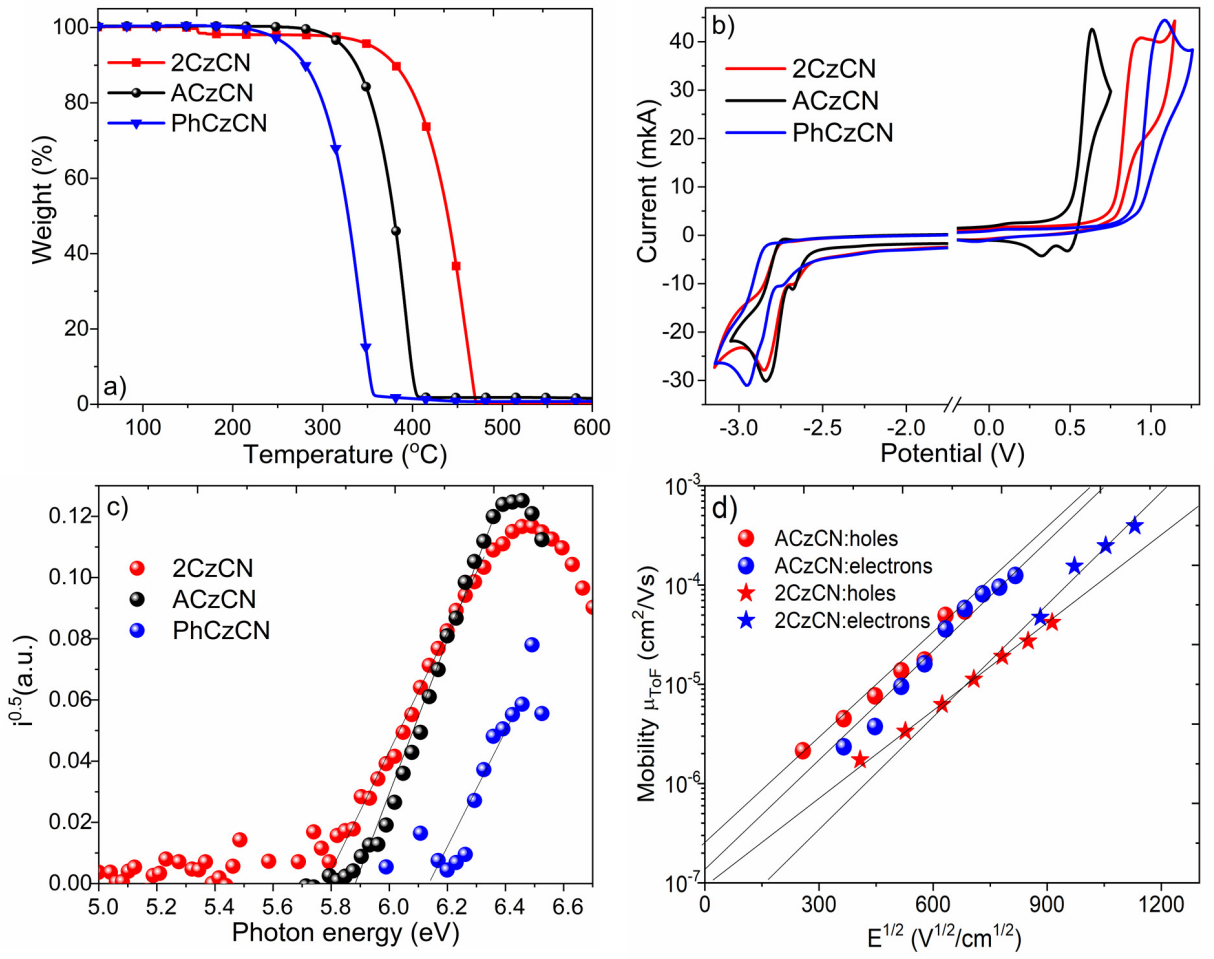

Fig. 2. TGA curves (a); CV voltammograms (b); photoelectron emission spectra (c) and hole- and electron- drift mobilities (d) of compounds 2CzCN, ACzCN and PhCzCN.

Table 1
Thermal and electrochemical characteristics of cyanocarbazolyl derivatives.

Compound	T_g,[a] [°C]	T_m,[a] [°C]	T_{cr},[a] [°C]	$T_{d\text{-}5\%}$,[b] [°C]	E^{ox}_{onset}, [V]	E^{red}_{onset}, [V]	IP_{CV} [eV]	EA_{CV} [eV]	$E_{g,\,CV}$ [eV]	IP_{PE} [eV]	EA_{PE} [eV]	$E_{g,\,opt}$ [eV]
2CzCN	101	222	–	362	0.77	−2.58	5.58	2.22	3.36	5.80	2.42	3.38
ACzCN	–	253	188	325	0.53	−2.59	5.33	2.21	3.12	5.85	2.45	3.39
PhCzCN	42	133	–	261	0.90	−2.58	5.70	2.22	3.48	6.12	2.72	3.40

T_g is the glass transition temperature; T_m is the melting point; T_{cr} is the crystallization temperature; $T_{d\text{-}5\%}$ is the temperature of 5% weight loss.
$E^{ox}_{onset}/E^{red}_{onset}$ is the onset of the first oxidation/reduction waves; IP_{CV}, EA_{CV} is the ionization potential and electron affinity, calculated using relationships $IP_{CV} = |e|(4.8 + E^{ox}_{onset})$ and $EA_{CV} = |e|(4.8 + E^{red}_{onset})$; IP_{PE} is the ionization potential obtained from the photoelectron emission spectra; EA_{PE} calculated by equation $EA_{PE} = IP_{PE}\text{-}E_{g,\,opt}$; $E_{g,\,opt}$ is the optical band gap ($E_g = 1240/\lambda_{abs,\,onset}$).
[a] Estimated from DSC.
[b] Estimated from TGA.

[35–37]. 2CzCN, ACzCN and PhCzCN were mixed with electron-accepting PO-T2T in molar ratio of 1:1. The formation of CT complexes at the ground state was not evident from UV spectra since the shapes and positions of absorption bands of exciplex systems are similar to the absorption spectra of individual donors and PO-T2T acceptor (Fig. S4a and Fig S11). Exciplex-forming blends displayed typically CT, broad, Gaussian-shaped emission spectra (Fig. 3c). The PL profiles of the films of molecular mixtures were clearly red-shifted relatively to the spectra of the films of individual molecules (Fig. 3c) and PO-T2T electron-acceptor (Fig. S11). The wavelengths of maxima of exciplex emission are in good agreement with difference between the HOMO level of the corresponding donors and LUMO energy (3.5 eV) of electron-accepting molecule PO-T2T (HOMO levels of the compounds were estimated from ultraviolet photoelectron spectroscopy for solid films and LUMO energy of PO-T2T was obtained subtracting the optical energy gap from the HOMO [38]). Compounds 2CzCN, ACzCN and PhCzCN possessed relatively high IP_{PE} values of 5.80, 5.85 and 6.13 eV, respectively, estimated from photoelectron emission spectra. PhCzCN with the highest IP_{PE} value of 6.13 eV exhibited the most blue-shifted exciplex emission (cyan) peaked at 494 nm in pair with PO-T2T (Table 2). Exciplex blend of ACzCN with PO-T2T showed yellow exciplex emission with the intensity maximum at 552 nm. The exciplex blend of 2CzCN with PO-T2T displayed greenish PL (509 nm).

PL and PH measurements were carried out at 77 K for estimation of the energy of excited states of bimolecular systems (Fig. 3c). Negligible $\Delta E_{S\text{-}T}$ values of 0.01–0.06 eV were obtained

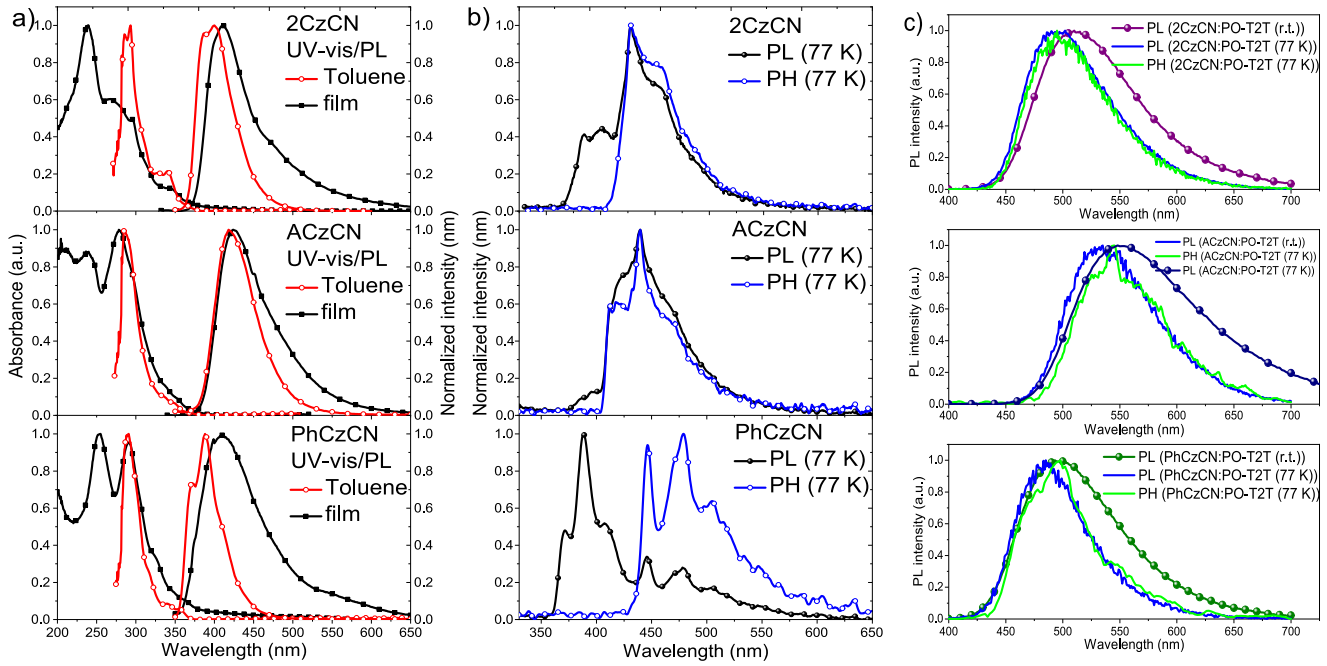

Fig. 3. (a) Absorption and fluorescence spectra of dilute toluene solutions (10^{-5} M) of compounds 2CzCN, ACzCN and PhCzCN along with (b) photoluminescence (PL) and phosphorescence (PH) spectra (with delay of > 50 ms) of THF solutions (10^{-5} M) recorded at 77 K. (c) PL spectra (r.t.) and PH spectra (77 K, 50 μs delay) of the films exciplex systems and constituting compounds (λ_{exc} = 330 nm).

Table 2
Photophysical characteristics of compounds 2CzCN, ACzCN and PhCzCN and their solid mixtures with PO-T2T.

Compound	λ_{abs} [b], [nm]	λ_{PL}, [nm]	PLQY[b], [%]	E_S, [eV]	E_T, [eV]	ΔE_{S-T}, [eV]	τ_1 (χ^2) [a] [ns]	$\tau^1/\tau^2/\tau^3$ (χ^2) [b] [ns]
2CzCN	363	396[a]/410[b]	15	3.34	3.03	0.31	5.04 (1.001)	1.35 (29%)/7.79(71%) (1.069)
ACzCN	378	422[a]/424[b]	7	3.33	3.04	0.29	4.46 (1.246)	0.92 (59%)/5.54(41%) (1.057)
PhCzCN	373	371, 387[a]/407[b]	11	3.45	2.90	0.55	8.50 (1.108)	0.80 (86%)/8.96(14%) (1.219)
2CzCN:PO-T2T	–	509[b]	15	2.83	2.82	0.01	–	28 (13%)/902 (23%)/ 3045 (64%) (1.272)
ACzCN:PO-T2T	–	552[b]	14	2.62	2.56	0.06	–	42(9%)/1113(44%)/ 2865 (47%) (1.232)
PhCzCN:PO-T2T	–	494[b]	37	2.87	2.86	0.01	–	39(6%)/4288(94%)/- (1.104)

λabs is the onset of the last absorption band; λ_{PL} is the fluorescence maxima; E_S, E_T are the energies of the first excited singlet and triplet states, estimated from the photoluminescence and phosphorescence measurements at 77 K (50 μ delay) and calculated by using the equation $E_S = 1240/\lambda_{onset,\ PL}$, $E_T = 1240/\lambda_{onset,\ PH}$; ΔE_{S-T} – singlet–triplet energy splitting; $\tau_1/\tau_2/\tau_3$ are the PL lifetimes. The decay profiles were fitted with residual values of 1.104–1.272.

[a] Measured for dilute toluene solutions (10^{-5}) of compounds.

[b] Measured for solid films of compounds.

Table 3
EL parameters of OLEDs.

Device	Donor (Spacer)	EL λ_{max},[a] nm	Turn on voltage V_{ON}, V	Luminescence max, cd/m^2	Max. CE, cd/A	Max. PE, lm/W	Max. EQE, %	CIE1931,[a] (x, y)
HAT-CN (10 nm)/TCTA (36 nm)/**Donor**(8 nm)/**Donor**:PO-T2T(24 nm)/PO-T2T(8 nm)/TPBi(36 nm)/LiF/Al								
A	2CzCN	504	5.2	25,700	23.6	9.6	7.7	(0.23, 0.43)
B	ACzCN	533	5.9	27,600	21.5	9	6.4	(0.33, 0.58)
C	PhCzCN	496	5.1	19,200	14.7	5.5	4.5	(0.26,0.51)
HAT-CN(10 nm)/TCTA (36 nm)/ 4CzTPN-Ph (1 nm)/**Donor**(8 nm)/**Donor**:PO-T2T(24 nm)/PO-T2T(8 nm)/TPBi(36 nm)/LiF/Al								
D	2CzCN	504	4.4	28,500	14.7	6.7	5	(0.25, 0.49)
E	ACzCN	529	5.6	23,000	22.4	10.2	6.5	(0.31, 0.57)
F	PhCzCN	494/577	5.8	20,000	7.8	2.9	3.1	(0.36, 0.44)

[a] at applied voltage of 9 V.

(Table 2). To screen delayed fluorescence properties of the exciplex mixtures, PL decay curves of the blends of 2CzCN, ACzCN and PhCzCN with PO-T2T were recorded at 300 K (Fig. 4a). Unlike the individual compounds, with their prompt fluorescence, in pair with PO-T2T, exciplex systems exhibited short- and long-lived components. It is well known that photophysics of exciplex-forming

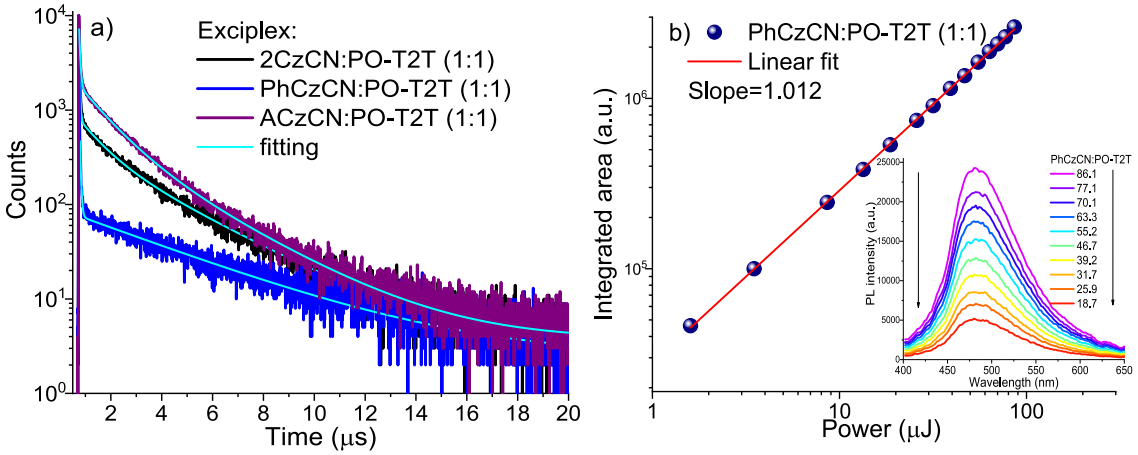

Fig. 4. (a) PL decay curves of exciplex-forming blends at 300 K and (b) integrated DF area as a function of the excitation dose (λ_{exc} = 330 nm) with 1 μs delay (inserted: PL spectra) of PhCzCN:PO-T2T exciplex system recorded at room temperature (λ_{exc} = 330 nm).

systems is much more complex than that of individual compounds exhibiting intramolecular CT nature [39]. As shown at Fig. 4a, exciplex-forming mixtures exhibited complex PL decays which could only be described by multi-exponential fittings (Table 2). Thus, at room temperature the exciplex systems of 2CzCN:PO-T2T and ACzCN:PO-T2T experienced tri-exponential PL decays. PL decay curve of the film of mixture PhCzCN:PO-T2T was well-fitted by bi-exponential function. The complex multi-exponential decays can be explained by the different distribution of exciplexes in the molecular blends with the different molecular geometries and arrangements.

To gain an insight into the nature of delayed fluorescence, time-resolved emission spectra were recorded and PL decay measurements at different temperatures were performed. The normalized emission spectra of exciplexes with different delay times recorded at room temperature are shown in Fig. S5. The spectra did not shift by setting different delay times of 800 ns, 1 μs, 2 μs, 4 μs and 8 μs. This observation indicates the presence of energetically stable charge transfer state. The molecular mixture of PhCzCN with PO-T2T showed delayed fluorescence only at the delay time of 800 ns and 1 μs. In all cases, the clearly separated rapid decay of prompt fluorescence was recorded along with the pronounced long-lived delayed fluorescence. The prompt fluorescence was not temperature-dependent, displaying the same shape and position of the spectra from 77 K up to 300 K (Fig. 4b, S6). Meanwhile, the long-lived delayed fluorescence (DF) and PH components displayed strong temperature dependence (Fig. S6). Ultra-long-lived component observed at low temperatures is assigned to the intensive triplet emission, i.e., phosphorescence. The decay curves were found to be similar over the temperature range of 77–140 K, in which PH dominated. With the increase of the temperature, the ultra-long-lived component gradually decreased and DF with long-lived component markedly activated. The DF observed at higher temperatures (180–300 K) can be assigned to TADF. This assumption was supported by the small singlet–triplet energy splitting ca. 0.01 eV of exciplex systems of and thus activated rISC process [1] (Table 2). Noteworthy, the positions of the spectra did not change in all range of the temperatures for all exciplex-forming systems (Fig. S6 (right)). To confirm the TADF nature of the emission, the intensity dependence of DF as the function of laser pulse energy was plotted (Fig. 4b, Fig. S7). For all three exciplex-forming systems, the linear relationship with the slope close to 1 was observed. This value of slope confirms that TADF process is responsible for DF [1].

Exciplex emission based organic light-emitting diodes

Capability of formation of exciplexes through a spacer was investigated partly by testing electroluminescent properties of the developed exciplex TADF exhibiting emitters. Using donors 2CzCN, ACzCN, PhCzCN, OLEDs A, B and C respectively were fabricated with the general structure HAT-CN (10 nm)/TCTA (36 nm)/Donor(8 nm)/Donor:PO-T2T (1:1) (24 nm)/PO-T2T(8 nm)/TPBi(36 nm)/LiF/Al (Fig. 5a, Table 3). The layers of HAT-CN and LiF played their usual roles of hole- and electron-injecting layers, respectively. Aiming to fix the charge recombination zone within exciplex-forming light-emitting layers of 2CzCN:PO-T2T, ACzCN:PO-T2T or PhCzCN:PO-T2T and to forbid interface exciplex formation with hole and electron transporting layers (TCTA and TPBi), the non-doped layers Donor (2CzCN, ACzCN or PhCzCN for device A, B or C, relatively) and PO-T2T were deposited. Since the thickness of the Donor layer was only 8 nm which was smaller than diffusion lengths of triplet excitons [40], transfer of triplet excitons through this layer could be expected. To check this assumption and to use it for obtaining white electroluminescence, OLEDs with the structure HAT-CN (10 nm)/TCTA (36 nm)/ 4CzTPN-Ph (1 nm)/Donor(8 nm)/Donor:PO-T2T (1:1) (24 nm)/PO-T2T(8 nm)/TPBi(36 nm)/LiF/Al were fabricated and named as devices D, E and F, respectively (Fig. 5a, Table 3). The layer of 4CzTPN-Ph was selected due to its efficient intramolecular TADF in orange range [1]. To provide precise comparison of the characteristics of the fabricated devices, the same layers were deposited at the same time for all the devices.

Broad EL spectra with a single band were recorded for devices A-C (Fig. 5b). The shape of the spectra did not change under the different voltages (Fig. S8). The electroluminescence of devices A-C can be attributed to emission of the volume exciplexes 2CzCN:PO-T2T, ACzCN:PO-T2T or PhCzCN:PO-T2T. Electroluminescence spectra were similar to the corresponding PL spectra (Fig. 3c). Low-intensity blue bands which may be related to emission of TCTA and/or TPBi were not detectible even at high voltages. Thus, recombination zones were located only within light-emitting layers due to the presence of electron- and hole-blocking layers of 2CzCN, ACzCN or PhCzCN and PO-T2T, respectively (Fig. 6a inset, S8). EL spectra of devices D and E were very similar to EL spectra of devices A and B since charge recombination occurred in the same light-emitting layers of 2CzCN:PO-T2T or ACzCN:PO-T2T, respectively (Fig. 5b). Presence of the layer of 4CzTPN-Ph in the structures of devices D and E did not show any effect on their EL

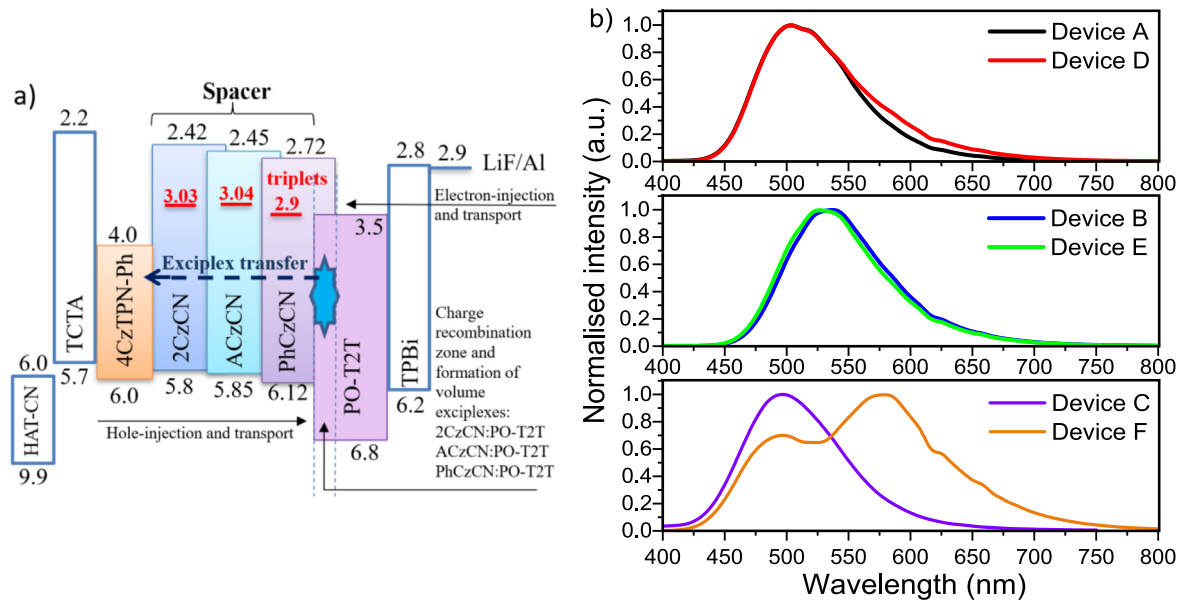

Fig. 5. (a) Equilibrium energy diagram where the energies are given in eV and (b) EL spectra at 9 V of the devices A-F.

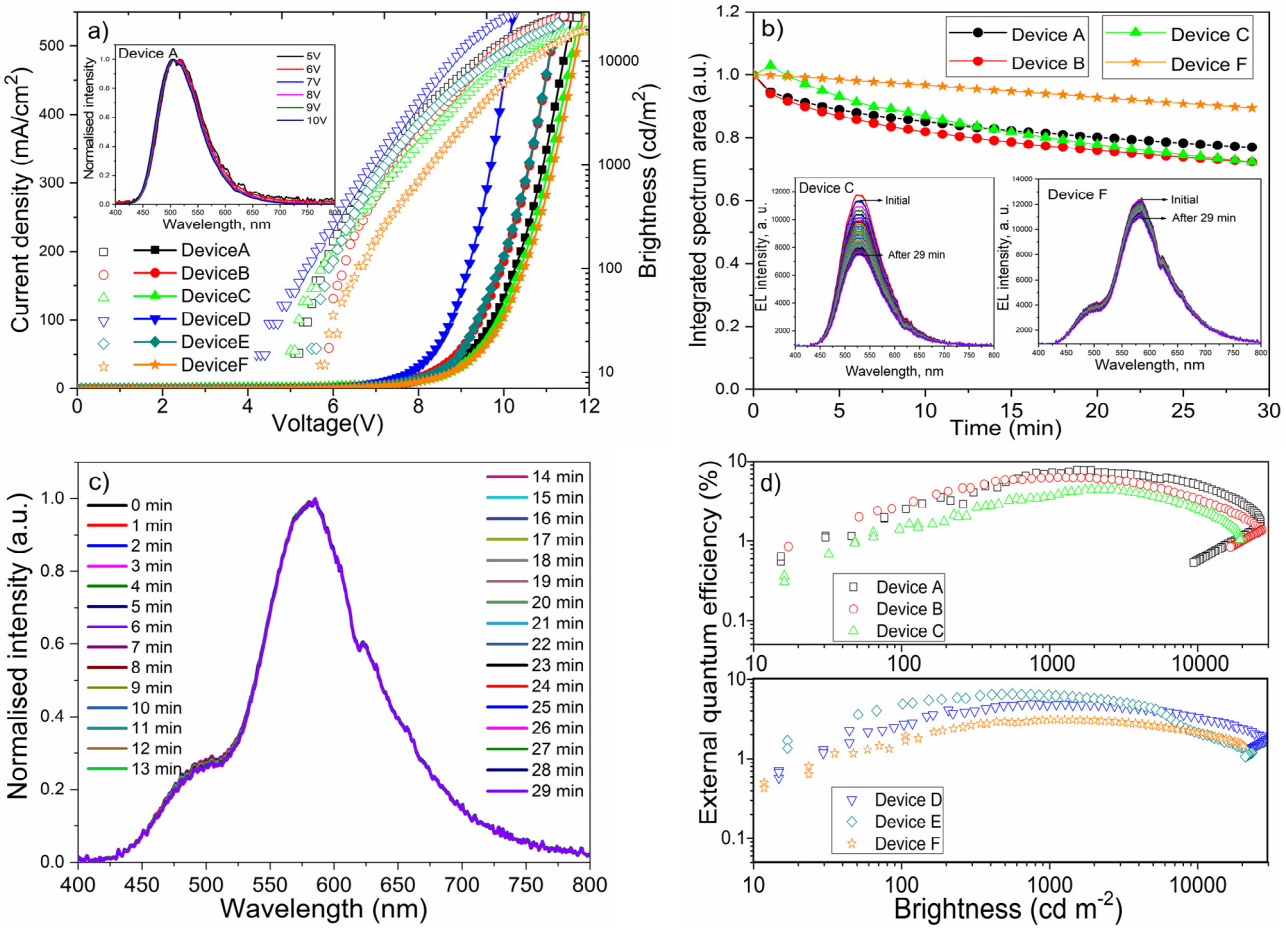

Fig. 6. Voltage–current density characteristics (inset shows EL spectra of device A at different applied voltages) of the designed devices A-F (a). Relative lifetime of the selected devices under constant voltage of 6 V (Insets: EL spectra of **PhCzCN**:PO-T2T-based devices C and F) (b); and EL spectra of the device F recorded with the step of 1 min under constant voltage of 6 V (c). EQE versus brightness of the fabricated devices (d).

spectra. In contrast, two corresponding bands at 494 and 577 nm which are attributed to cyan PhCzCN:PO-T2T and orange 4CzTPN-Ph emissions were observed in EL spectrum of device F (Fig. 5b, Fig. 3c) [22]. Direct hole-electron recombination did not take place in the layer of 4CzTPN-Ph due to the significant energy barrier (0.78 eV) between PO-T2T and PhCzCN which is also in

agreement with the absence of TCTA emission from the reference device C (Fig. 5 a, b). Thus, orange emission of 4CzTPN-Ph indicates the exciplex energy transfer through the spacer layer of PhCzCN (8 nm) as it is schematically shown in Fig. 5a.

Since exciplex energy transfer through the spacer did not occur in case of the reference devices D and E with the spacer layers of 2CzCN (8 nm) and ACzCN (8 nm), the mechanism of the exciplex energy transfer trough the spacer in the system 4CzTPN-Ph/PhCzCN/PhCzCN:PO-T2T can be attributed to both the spacer PhCzCN and exciplex forming mixture PhCzCN:PO-T2T. Taking into account that the diffusion lengths of triplet excitons can be up to ca. 15 nm [35], the exciplex (triplet exciplex) energy transfer through the spacer PhCzCN (but not through the spacers 2CzCN and ACzCN) can be explained taking into account lower triplet energy level of PhCzCN (2.9 eV) than that of 2CzCN (3.03 eV) and ACzCN (3.04 eV) (Fig. 5a, 3b, Table 2). Interestingly, exciplex energy transfer through the spacer was observed even when the thickness of the sparer layer of PhCzCN was increased up to 25 nm and red iridium complex Ir(piq)$_2$(acac) was used in the reference device F1 with the structure ITO/HAT-CN (10 nm) /TCTA(40 nm) / Ir(piq)$_2$(acac) (1 nm) /donor (25 nm) /donor:PO-T2T (20 nm) /PO-T2T (40 nm) /LiF/Al (Fig. S9). Expectedly, the exciplex energy transfer through the spacer was not observed for devices D1 and E1 based on the spacer-exciplex systems 2CzCN/2CzCN:PO-T2T and ACzCN/ACzCN:PO-T2T similarly to that of devices D and E based on the same spacer-exciplex systems (Fig. S9). The triplet diffusion was not expected on the distance of 25 nm. Apparently, it could happen only for unique spacer-exciplex systems PhCzCN/PhCzCN:PO-T2T.

At first sight, assuming that the Förster self-radius (R_0) in the PhCzCN:PO-T2T blend is larger than thicknesses of the spacer PhCzCN (8 nm), the long-range Förster energy transfer (FRET) may be a reason of the observed EL behavior of the device F similarly to that observed for many conventional TADF based systems (Fig. 7) [22,23,25]. If R_0 in 2CzCN:PO-T2T and ACzCN:PO-T2T blends is lower than R_0 of PhCzCN:PO-T2T (which is expected since PLQY of PhCzCN:PO-T2T exciplex emission is higher than PLQY of emissions of exciplexes 2CzCN:PO-T2T and ACzCN:PO-T2T (Table 2)), FRET could not be detected in the reference devices D and E explaining the different EL behavior of devices D-F. Indeed, R_0 in organic amorphous films is typically several nanometers which is somehow comparable with the thickness (d) of the spacer used in devices D-F (e.g. 1.9 nm for NPB and 2.2 nm for CBP [41]; or 7.4 nm for TTPA and 8.5 nm for DBP [25]). However, the energy transfer through the spacer of device F was observed even when the thickness of the sparer layer was of 25 nm which is apparently longer distance within which FRET can occur (Figure S9). In addition, very thin layers of 4CzTPN-Ph (of 1 nm) were used in the structures of devices D-F and 4CzTPN-Ph is characterized by relatively weak ICT absorption band in the range of emission of exciplexes PhCzCN:PO-T2T, 2CzCN:PO-T2T and ACzCN:PO-T2T [26]. Thus, absorbance of the layer of 4CzTPN-Ph should be not strong enough for FRET. Therefore, we looked for alternative explanation of working mechanism of device F.

It is known that triplet exciton diffusion length in organic semiconductors is of tens of nanometers, i.e. it is much longer than singlet exciton diffusion length. e.g., singlet diffusion length of ca. 5 nm [42] and triplet diffusion length of ca. 87 nm were obtained for amorphous layers of NPB [43]). Taking this into account, the working mechanism of device F can be explained by the case 2 shown in Fig. 7. In case of device F, the exciplex (triplet exciplex) energy transfer through the spacer occurred resulting in EL of both PhCzCN:PO-T2T exciplex (marked as λ_1) and TADF of 4CzTPN-Ph (marked as λ_2) when thickness of spacer d > R_0 (no FRET) and no energy barrier between triplet energy levels of PhCzCN:PO-T2T exciplex and spacer PhCzCN (ΔE_{TT} was small). In case of the reference devices D and E, the exciplex (triplet exciplex) energy transfer through the spacer did not occur resulting in single color EL (λ_1) because of high energy barrier ΔE_{TT}.

The possible reason of that can be resonance (similarities) between triplet energy levels of spacer **PhCzCN** (2.9 eV) and exciplex **PhCzCN**:PO-T2T (2.86 eV). Because of the relatively big differences between triplet energies of **2CzCN** and **2CzCN**:PO-T2T (0.47 eV) as well as of **ACzCN** and **ACzCN**:PO-T2T (0.18 eV) (Fig. 3b, c, Table 2), the exciplex energy transfer through the spacer was not observed for devices D, E, D1, E1. (Fig. 5b, S9). As a result of the long-distance exciplex energy transfer through the spacer in the system 4CzTPN-Ph/**PhCzCN**/**PhCzCN**:PO-T2T, warm white electroluminescence with the CIE coordinates of (0.36, 0.44) at 9 V was observed for device F (Fig. 5b, Table 3). In addition, stability of device F was improved in comparison to that of only exciplex-based device C (Fig. 6b). From the first glance, it can seem that stability of this device F can be improved due to usage of more stable orange emitter 4CzTPN-Ph. However, there are no big differences between stability of cyan exciplex **PhCzCN**:PO-T2T and orange 4CzTPN-Ph. This conclusion is based on the stability of normalized EL spectra of device F under continuous electrical excitation during 29 min (Fig. 6c).

Apparently, the high-energy triplet exciplexes mainly take part in the exciplex transfer when the resonance between triplet energy levels of exciplex and spacer occurs. This can lead to the decrease of number of "hot" excitons and/or "hot" polarons in the light-emitting layer of **PhCzCN**:PO-T2T which are usually formed when the long-lived triplets are present in phosphorescent and TADF emitters [44,45]. Thus, having the exciplex transfer, lifetime of TADF-exciplex-based device F was increased (Fig. 6b). It should be noted that high maximum external quantum efficiencies (EQE) up to 7.7% were obtained for exciplex-based devices A-C overcoming the theoretical limit (ca. 5% [46]) of simple fluorescent devices (Fig. 6d, Table 3). Such EQE values are slightly higher than those of previously reported exciplex-based devices with a cyanocarbazolyl-based derivatives used as acceptors [15]. However, maximum EQE values of **2CzCN**:PO-T2T, **ACzCN**:PO-T2T, **PhCzCN**:PO-T2T-based devices A-C are ca. twice lower than maximum EQE (16%) of cyan CN-Cz2:PO-T2T-based device, where 9-phenyl-9*H*-3,9'-bicarbazole-6-carbonitrile (CN-Cz2) was used as donor [14]. In addition, CN-Cz2:PO-T2T-based device showed much lower turn-on voltage (2.3 V) than turn-on voltages (5.1–5.9 V) obtained for devices A-C (Table 3). The additional modification of device structure may help to improve electroluminescent properties of OLEDs based on emission of exciplexes **2CzCN**:PO-T2T, **ACzCN**:PO-T2T, **PhCzCN**:PO-T2T, for example, by doping of additional layers as it was used for the CN-Cz2:PO-T2T-based device [14]. Meanwhile, maximum brightness of the all fabricated devices was much higher than 10000 cd/m^2 which is in good agreement with the abovementioned efficient device based on the TADF exciplex CN-Cz2:PO-T2T (Table 3) [14]. The maximum EQEs of devices D-F are slightly lower than those of the corresponding devices A-C apparently because of the loss of charge currier balance after addition of the layer of the layer of 4CzTPN-Ph. Nevertheless, the obtained results demonstrate the mechanism of the exciplex transfer which can be used for both enhancement of device stability and for obtaining of white electroluminescence.

Conclusion

Selective long-distance exciplex energy transfer through the spacer under electrical excitation was observed for the exciplex forming mixture-spacer system based on the same acceptor and

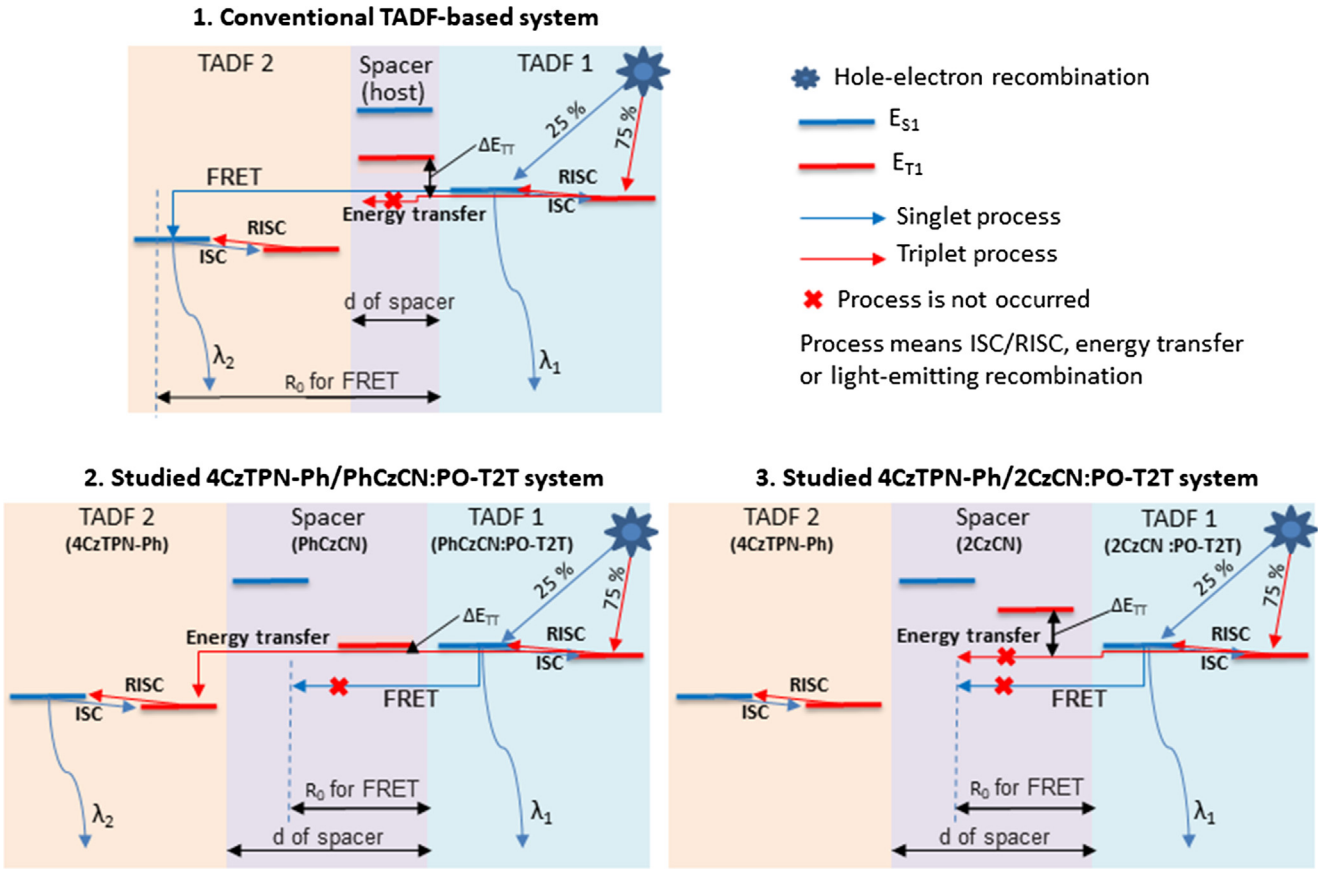

Fig. 7. Schematic representation of the energy diagram for conventional TADF-based systems (case 1, where d < R_0 and ΔE_{TT} is high) and the studied ones (case 2, where d > R_0 and ΔE_{TT} is small and case 3, where d > R_0 and ΔE_{TT} is high).

on one of specially designed here donors used as exciplex-forming material and as the spacer. Such selectivity of the exciplex energy transfer is explained by the resonance of triplet energy levels between exciplex and spacer. The exciplex energy transfer in the structures of organic light-emitting diodes can be utilized for both improving of device stability and for getting white electroluminescence. Efficient single-color and white devices with new exciplex-forming systems were fabricated achieving external quantum efficiency of 7.7%. The warm white electroluminescence with CIE coordinates of (0.36, 0.44) was observed exploiting cyan intermolecular (exciplex) and orange intramolecular thermally activated delayed fluorescence.

Compliance with Ethics Requirements

This article does not contain any studies with human or animal subjects.

Declaration of Competing Interest

The authors declare that they have no known competing financial interests or personal relationships that could have appeared to influence the work reported in this paper.

Acknowledgements

This work was supported by the Research Council of Lithuania (Project "OWEX", No S-MIP-17-101).

Appendix A. Supplementary data

Supplementary data to this article can be found online at https://doi.org/10.1016/j.jare.2020.04.018.

References

[1] Goushi K, Yoshida K, Sato K, Adachi C. Organic light-emitting diodes employing efficient reverse intersystem crossing for triplet-to-singlet state conversion. Nat Photonics 2012;6:253–8. doi: https://doi.org/10.1038/nphoton.2012.31.
[2] Jankus V, Data P, Graves D, McGuinness C, Santos J, Bryce MR, et al. Highly efficient TADF OLEDs: How the emitter-host interaction controls both the excited state species and electrical properties of the devices to achieve near 100% triplet harvesting and high efficiency. Adv Funct Mater 2014;24:6178–86. doi: https://doi.org/10.1002/adfm.201400948.
[3] Liu Y, Li C, Ren Z, Yan S, Bryce MR. All-organic thermally activated delayed fluorescence materials for organic light-emitting diodes. Nat Rev Mater 2018;3:1–20. doi: https://doi.org/10.1038/natrevmats.2018.20.
[4] Kim BS, Lee JY. Engineering of mixed host for high external quantum efficiency above 25% in green thermally activated delayed fluorescence device. Adv Funct Mater 2014;24:3970–7. doi: https://doi.org/10.1002/adfm.201303730.
[5] Cho YJ, Yook KS, Lee JYA. Universal host material for high external quantum efficiency close to 25% and long lifetime in green fluorescent and phosphorescent OLEDs. Adv Mater 2014;24:4050–5. doi: https://doi.org/10.1002/adma.201400347.
[6] Kotadiya NB, Blom PWM, Wetzelaer G-JAH. Efficient and stable single-layer organic light-emitting diodes based on thermally activated delayed fluorescence. Nat Photonics 2019;13:765–9. doi: https://doi.org/10.1038/s41566-019-0488-1.
[7] Chapran M, Pander P, Vasylieva M, Wiosna-Salyga G, Ulanski J, Dias FB, et al. Realizing 20% external quantum efficiency in electroluminescence with efficient thermally activated delayed fluorescence from an exciplex. ACS Appl Mater Interfaces 2019;11:13460–71. doi: https://doi.org/10.1021/acsami.8b18284.
[8] Zhang M, Liu W, Zheng C-J, Wang K, Shi Y-Z, Li X, et al. Tricomponent exciplex emitter realizing over 20% external quantum efficiency in organic light-

emitting diode with multiple reverse intersystem crossing channels. Adv Sci 2019;1801938:1–9. doi: https://doi.org/10.1002/advs.201801938.
[9] Wu T-L, Liao S-Y, Huang P-Y, Hong Z-S, Huang M-P, Lin C-C, et al. Exciplex organic light-emitting diodes with nearly 20% external quantum efficiency: effect of intermolecular steric hindrance between the donor and acceptor pair. ACS Appl Mater Interfaces 2019;11:19294–300. doi: https://doi.org/10.1021/acsami.9b04365.
[10] Zhong P-L, Zheng C-J, Zhang M, Zhao J-W, Yang H-Y, He Z-Y, et al. Highly efficient ternary polymer-based solution-processable exciplex with over 20% external quantum efficiency in organic light-emitting diode. Org Electron 2020;76:. doi: https://doi.org/10.1016/j.orgel.2019.105449105449.
[11] Zhao J, Zheng C, Zhou Y, Li C, Ye J, Du X, et al. Novel small-molecule electron donor for solution-processed ternary exciplex with 24% external quantum efficiency in organic light-emitting diode. Mater Horiz 2019;6:1425–32. doi: https://doi.org/10.1039/C9MH00373H.
[12] Cekaviciute M, Simokaitiene J, Volyniuk D, Sini G, Grazulevicius JV. Arylfluorenyl-substituted metoxytriphenylamines as deep blue exciplex forming bipolar semiconductors for white and blue organic light-emitting diodes. Dyes Pigm 2017;140:187–202. doi: https://doi.org/10.1016/j.dyepig.2017.01.023.
[13] Hung WY, Fang GC, Lin SW, Cheng SH, Wong KT, Kuo TY, et al. The first tandem, all-exciplex-based WOLED. Sci Rep 2015;4:4–9. doi: https://doi.org/10.1038/srep05161.
[14] Lin Tzu-Chieh, Sarma Monima, Chen Yi-Ting, Liu Shih-Hung, Lin Ke-Ting, Chiang Pin-Yi, Chuang Wei-Tsung, Liu Yi-Chen, Hsu Hsiu-Fu, Hung Wen-Yi, Tang Wei-Chieh, Wong Ken-Tsung, Chou Pi-Tai. Probe exciplex structure of highly efficient thermally activated delayed fluorescence organic light emitting diodes. Nat Commun 2018;9(1). doi: https://doi.org/10.1038/s41467-018-05527-4.
[15] Sarma M, Wong K-T. Exciplex: An intermolecular charge-transfer approach for TADF. ACS Appl Mater Interfaces 2018;10:19279–304. doi: https://doi.org/10.1021/acsami.7b18318.
[16] Kim H-B, Kim J-J. Recent progress on exciplex-emitting OLEDs. J Inf Disp 2019;20:105–21. doi: https://doi.org/10.1080/15980316.2019.1650838.
[17] Grybauskaite-Kaminskiene G, Ivaniuk K, Bagdziunas G, Turyk P, Stakhira P, Baryshnikov G, et al. Contribution of TADF and exciplex emission for efficient "warm-white" OLEDS. J Mater Chem C 2018;6:1543–50. doi: https://doi.org/10.1039/c7tc05392d.
[18] Yao J, Ying S, Qiao X, Yang D, Chen J, Ahamad T, et al. High efficiency and low roll-off all fluorescence white organic light-emitting diodes by the formation of interface exciplex. Org Electron 2019;67:72–8. doi: https://doi.org/10.1016/j.orgel.2019.01.011.
[19] Zhao F, Wei Y, Xu H, Chen D, Ahamad T, Alshehri S, et al. Spatial exciton allocation strategy with reduced energy loss for high-efficiency fluorescent/phosphorescent hybrid white organic light-emitting diodes. Mater Horiz 2017;4:641–8. doi: https://doi.org/10.1039/C7MH00131B.
[20] Nakanotani H, Furukawa T, Morimoto K, Adachi C. Long-range coupling of electron-hole pairs in spatially separated organic donor-acceptor layers. Sci Adv 2016;2:. doi: https://doi.org/10.1126/sciadv.1501470e1501470.
[21] Pu Y-J, Koyama Y, Otsuki D, Kim M, Chubachi H, Seino Y, et al. Exciplex emissions derived from exceptionally long-distance donor and acceptor molecules. Chem Sci 2019;10:9203–8. doi: https://doi.org/10.1039/C9SC04262H.
[22] Nakanotani H, Higuchi T, Furukawa T, Masui K, Morimoto K, Numata M, et al. High-efficiency organic light-emitting diodes with fluorescent emitters. Nat Commun 2014;5:4016. doi: https://doi.org/10.1038/ncomms5016.
[23] Li Y, Wei Q, Cao L, Fries F, Cucchi M, Wu Z, et al. Organic light-emitting diodes based on conjugation-induced thermally activated delayed fluorescence polymers: Interplay between intra- and intermolecular charge transfer states. Front Chem 2019;7:688. doi: https://doi.org/10.3389/fchem.2019.00688.
[24] Skuodis E, Tomkeviciene A, Reghu R, Peciulyte L, Ivaniuk K, Volyniuk D, et al. OLEDs based on the emission of interface and bulk exciplexes formed by cyano-substituted carbazole derivative. Dyes Pigm 2017;139:795–807. doi: https://doi.org/10.1016/j.dyepig.2017.01.016.
[25] Higuchi T, Nakanotani H, Adachi C. High-Efficiency White organic light-emitting diodes based on a blue thermally activated delayed fluorescent emitter combined with green and red fluorescent emitters. Adv Mater 2015;27:2019–23. doi: https://doi.org/10.1002/adma.201404967.
[26] Uoyama H, Goushi K, Shizu K, Nomura H, Adachi C. Highly efficient organic light-emitting diodes from delayed fluorescence. Nature 2012;492:234–8. doi: https://doi.org/10.1038/nature11687.
[27] Matulaitis T, Kostiv N, Grazulevicius JV, Peciulyte L, Simokaitiene J, Jankauskas V, et al. Synthesis and properties of bipolar derivatives of 1,3,5-triazine and carbazole. Dyes Pigm 2016;127:45–58. doi: https://doi.org/10.1016/j.dyepig.2015.11.001.
[28] Tucker SH. LXXIV.-Iodination in the carbazole series. J Chem Soc 129 1926:546–53. doi: https://doi.org/10.1039/JR9262900546.
[29] Tomkeviciene A, Matulaitis T, Guzauskas M, Andruleviciene V, Volyniuk D, Grazulevicius JV. Thianthrene and acridan-substituted benzophenone or diphenylsulfone: effect of triplet harvesting via TADF and phosphorescence on efficiency of all-organic OLEDS. Org Electron 2019;70:227–39. doi: https://doi.org/10.1016/j.orgel.2019.04.025.
[30] Sworakowski J. How accurate are energies of HOMO and LUMO levels in small-molecule organic semiconductors determined from cyclic voltammetry or optical spectroscopy?. Synth Met 2018;235:125. doi: https://doi.org/10.1016/j.synthmet.2017.11.013.
[31] Galievsky VA, Druzhinin SI, Demeter A, Mayer P, Kovalenko SA, Senyushkina TA, et al. Ultrafast intramolecular charge transfer with *N*-(4-cyanophenyl)carbazole. Evidence for a le precursor and dual LE + ICT fluorescence. J Phys Chem A 2010;114:12622–38. doi: https://doi.org/10.1021/jp1070506.
[32] Brunner K, Dijken A, Börner H, Bastiaansen JJAM, Kiggen NMM, Langeveld BMW. Carbazole compounds as host materials for triplet emitters in organic light-emitting diodes: tuning the HOMO level without influencing the triplet energy in small molecules. J Am Chem Soc 2004;126:6035–42. doi: https://doi.org/10.1021/ja049883a.
[33] Holmes RJ, Forrest SR. Blue organic electrophosphorescence using exothermic host–guest energy transfer. Appl Phys Lett 2003;82:2422–4. doi: https://doi.org/10.1063/1.1568146.
[34] Rimkus R, Tumkevičius S, Serevičius T, Komskis R, Adomėnas P, Gruodis A, et al. Heterocyclic heptacene analogs – 8*H*–16,17-epoxydinaphto[2,3-*c*:2′,3′-*g*]carbazoles as charge transport materials. Dyes Pigm 2016;124:133–44. doi: https://doi.org/10.1016/j.dyepig.2015.08.029.
[35] He Z, Wang C, Zhao J, Du X, Yang H, Zhong P, et al. Blue and white solution-processed TADF-OLEDs with over 20% EQE, low driving voltages and moderate efficiency decrease based on interfacial exciplex hosts. J Mater Chem C 2019;7:11806–12. doi: https://doi.org/10.1039/C9TC03468D.
[36] Wei X, Gao L, Miao Y, Zhao Y, Yin M, Wang H, et al. A new strategy for structuring white organic light-emitting diodes by combining complementary emissions in the same interface. J Mater Chem C 2020;8:2772–9. doi: https://doi.org/10.1039/C9TC06198C.
[37] Feng D, Dong D, Lian L, Wang H, He G. High efficiency non-doped white organic light-emitting diodes based on blue exciplex emission. Org Electron 2018;56:216–20. doi: https://doi.org/10.1016/j.orgel.2018.02.016.
[38] Wu Z, Yu L, Zhao F, Qiao X, Chen J, Ni F, et al. Precise exciton allocation for highly efficient white organic light-emitting diodes with low efficiency roll-off based on blue thermally activated delayed fluorescent exciplex emission. Adv Optical Mater 2017;5(1700415):1–9. doi: https://doi.org/10.1002/adom.201700415.
[39] Graves D, Jankus V, Dias FB, Monkman AP. Photophysical investigation of the thermally activated delayed emission from films of m-MTDATA: PBD exciplex. Adv Funct Mater 2014;24:2343–51. doi: https://doi.org/10.1002/adfm.201303389.
[40] Luhman WA, Holmes RJ. Enhanced exciton diffusion in an organic photovoltaic cell by energy transfer using a phosphorescent sensitizer. Appl Phys Lett 2009;94:. doi: https://doi.org/10.1063/1.3120566153304.
[41] Lunt RR, Giebink NC, Belak AA, Benziger JB, Forrest SR. Exciton diffusion lengths of organic semiconductor thin films measured by spectrally resolved photoluminescence quenching. J Appl Phys 2009;105:. doi: https://doi.org/10.1063/1.3079797053711.
[42] Hofmann S, Rosenow TC, Gather MC, Lüssem B, Leo K. Singlet exciton diffusion length in organic light-emitting diodes. Phys Rev B 85 2012;245209. doi: https://doi.org/10.1103/PhysRevB.85.245209.
[43] Mikhnenko OV, Ruiter R, Blom PWM, Loi MA. Direct measurement of the triplet exciton diffusion length in organic semiconductors. Phys Rev Lett 2012;108:. doi: https://doi.org/10.1103/PhysRevLett.108.137401137401.
[44] Giebink NC, D'Andrade BW, Weaver MS, Mackenzie PB, Brown JJ, Thompson ME, et al. Intrinsic luminance loss in phosphorescent small-molecule organic light emitting devices due to bimolecular annihilation reactions. Int J Appl Phys 2008;103:. doi: https://doi.org/10.1063/1.2884530044509.
[45] Lee J, Jeong C, Batagoda T, Coburn C, Thompson ME, Forrest SR. Hot excited state management for long-lived blue phosphorescent organic light-emitting diodes. Nat Commun 2017;8:15566. doi: https://doi.org/10.1038/ncomms15566.
[46] Tsutsui T. Progress in electroluminescent devices using molecular thin films. MRS Bull 1997;22:39–45. doi: https://doi.org/10.1557/S0883769400033613.